

Optical interrogation of neural circuits in *Caenorhabditis elegans*

Zengcai V Guo, Anne C Hart & Sharad Ramanathan

Supplementary figures and text:

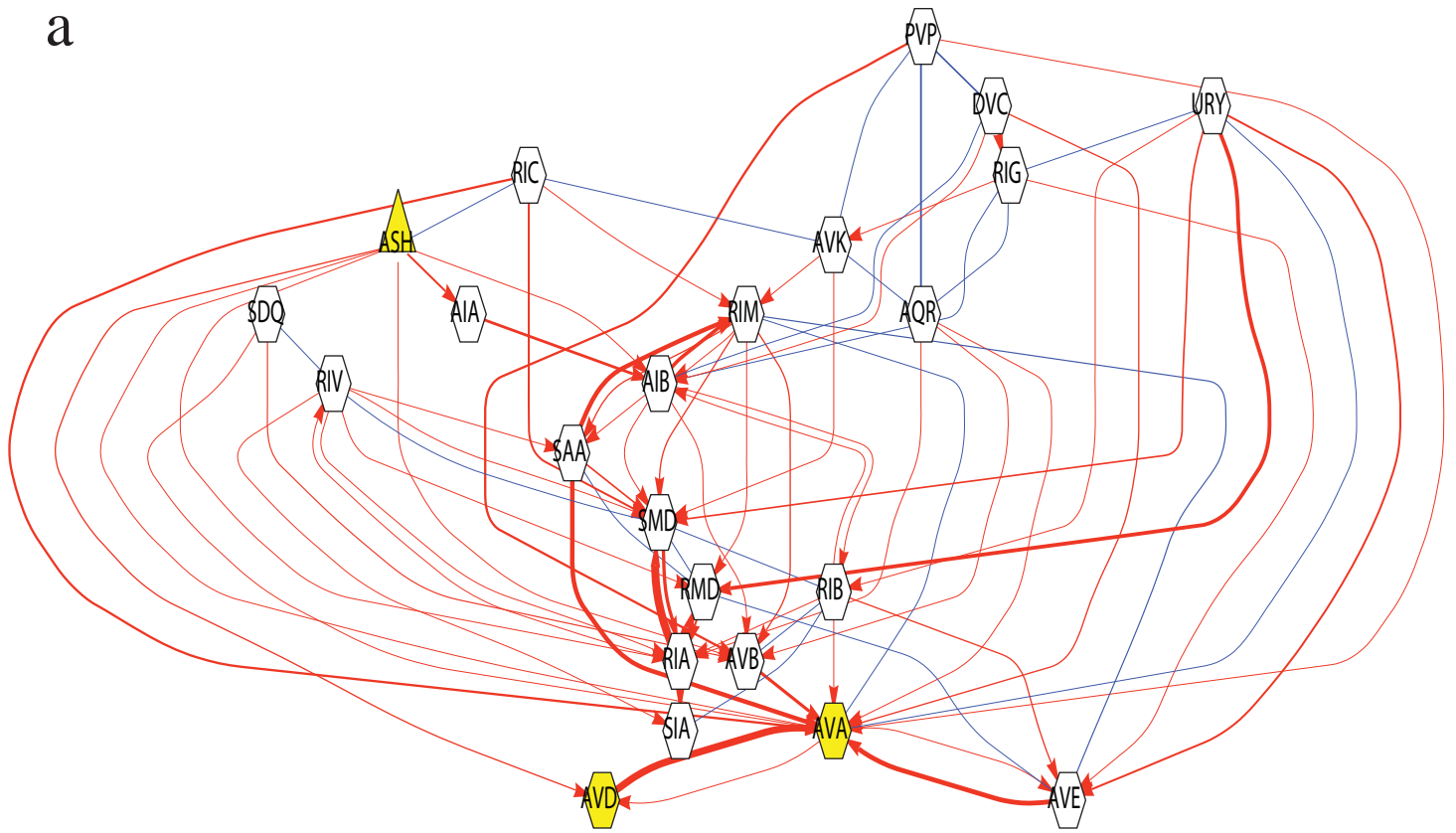
Supplementary Figure 1	Direct and indirect synaptic connections from ASH to AVA and AVD.
Supplementary Figure 2	Neuronal activity in AVA correlates with backward movement.
Supplementary Figure 3	Low laser intensity, 0.01mw/mm ² , can monitor G-CaMP fluorescence in AVA and AVD upon ASH activation.
Supplementary Figure 4	Specific stimulation of ASH activates AVA and AVD in <i>lite-1(ce314)</i> animals.
Supplementary Figure 5	Averaged G-CaMP traces in ASH and AVA upon ASH stimulation in <i>lite-1</i> , the wild type, <i>osm-3</i> and <i>eat-4</i> genetic background.
Supplementary Figure 6	Averaged G-CaMP traces in ASH and AVD upon ASH stimulation in the wild type, <i>lite-1</i> and <i>eat-4</i> genetic background.
Supplementary Figure 7	Specific stimulation of ASH in <i>lite-1(ce314)</i> animals cultivated without retinal resulted no activation in both ASH and AVA.
Supplementary Figure 8	Specific stimulation of ASH activates AVA and AVD in the wild type background.
Supplementary Figure 9	Stimulation of ASH can repeatedly activate AVA in the wild type background.
Supplementary Figure 10	Specific stimulation of ASH activates AVA and AVD in the <i>osm-3(p802)</i> background.
Supplementary Figure 11	Specific stimulation of ASH typically cannot activate AVA and AVD in the <i>eat-4(ky5)</i> background.
Supplementary Figure 12	Behavior analysis of ChR2 activation in RIM/ASH in <i>lite-1(ce314)</i> , <i>unc-9(fc16)</i> genetic background.
Supplementary Figure 13	Specific stimulation of RIM activates AVA in the wild type background.
Supplementary Figure 14	Specific stimulation of RIM activates AVA in the <i>lite-1(ce314)</i> background.
Supplementary Figure 15	Averaged G-CaMP traces in RIM and AVA upon RIM stimulation in wild type and <i>lite-1(ce314)</i> genetic background.
Supplementary Figure 16	Stimulating and monitoring neurons on different focal planes.
Supplementary Figure 17	The avoidance response generated by ChR2 activation in ASH in <i>lite-1(ce314)</i> background is blue light intensity dependent.
Supplementary Figure 18	The G-CaMP fluorescence intensity jump in neurons stimulated using blue light.
Supplementary Figure 19	Effects of choosing different number of pixels on the G-CaMP fluorescence trace.
Supplementary Figure 20	Illustration of movies.
Supplementary Table 1	Transgenic strains and their genotypes.
Supplementary Table 2	Primers used for PCR.
Supplementary Note	

Note: Supplementary Movies 1–6 are available on the Nature Methods website.

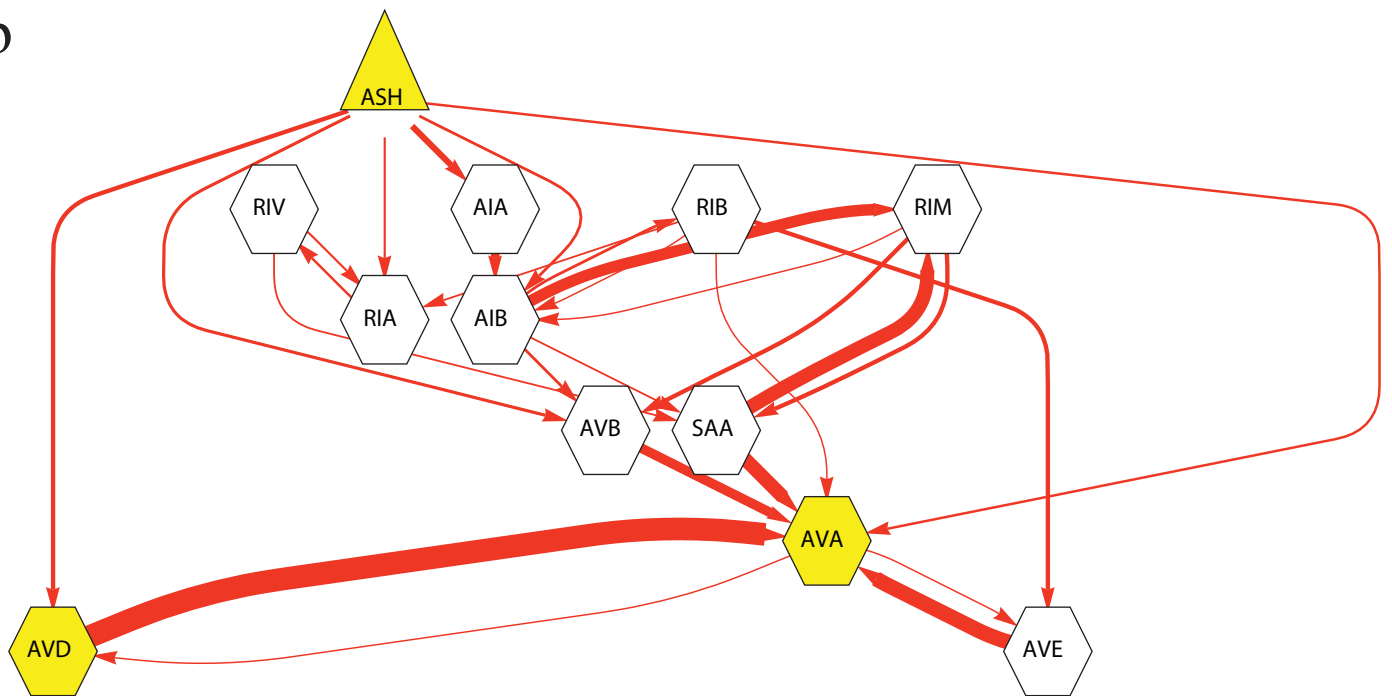
Supplementary Figure 1 | Direct and indirect synaptic connections from ASH to AVA and AVD. (a) The direct and potential important indirect synaptic connections from ASH to AVA and AVD. The connectivity data was from Chen et al¹. Potential important connections are defined as those with the number of synapses greater than a threshold. For chemical synapses (red), the threshold is half of the number of direct synapses between ASH and AVA. For gap junctions (blue), the threshold is half of the number of the gap junctions between RIM and AVA. The line thickness representing each connection is proportional to the number of chemical synapses and gap junctions, respectively. Among ASH's direct synaptic partners, only those express glutamate receptors or are connected to ASH through gap junctions are shown. Connections with more than four steps (more than three intermediate neurons) were not shown for simplicity. The same class of neurons was combined to plot the synaptic connections. We note that the connection between AIA and RIF, which was shown prominent in White et al², is not important here according to the criteria used here. (b) The gap junctions in (a) were removed to show the potential important connections in *unc-9* animals. The scale of line thickness representing chemical synapses is larger than in (a) for clarity. This figure highlights the importance of the indirect connections of ASH to AVA through AVB, AVE, RIB and SAA besides the direct connections from ASH to AVA and AVD.

Supplementary Figure 1

a



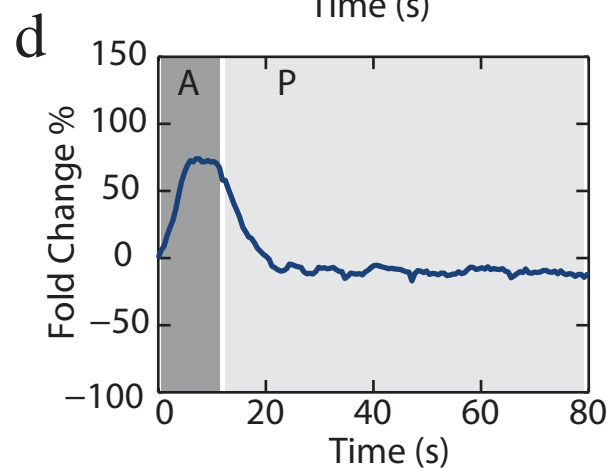
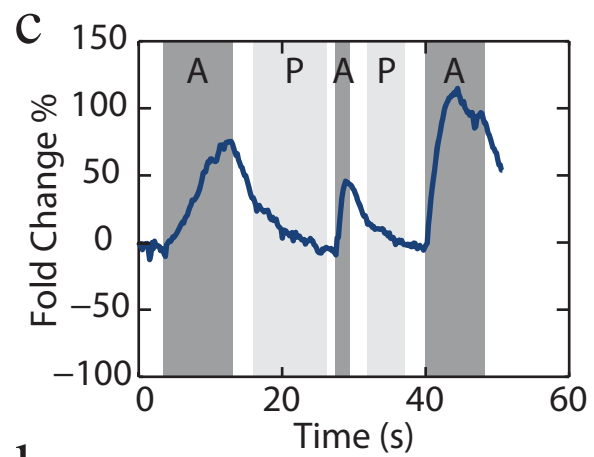
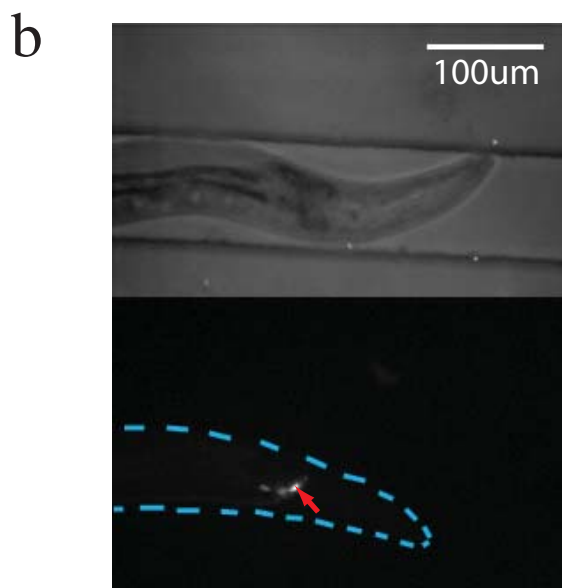
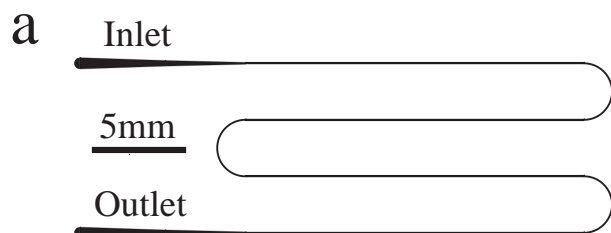
b



Supplementary Figure 2 | Neuronal activity in AVA correlates with backward movement.

(a) Design of the microfluidic device used to study neuronal activity in AVA. (b) Animal in the microfluidic device (top) with an AVA interneuron (bottom, indicated by red arrow, the animal was outlined by dashed curves). The microfluidic device was fabricated as described³. The animal expressed G-GCaMP in AVA using the extrachromosomal array *sraEx47 [nmr-1p::G-CaMP; unc-119(+)]*. (c) One representative trace of G-CaMP fluorescence intensity in AVA in the animal shown in (b). When worms move backward, they generate anterior propagating body waves. The anterior propagating (A) and posterior propagating (P) body waves were scored as described⁴. When body waves were switched between anterior propagating and posterior propagating, there was typically a period during which no travelling waves were generated. Thus the period for generating the anterior propagating or posterior propagating body waves is approximate. However, the neuronal activity in AVA qualitatively correlates with the reversals, consistent with previous results⁴. (d) A representative trace of G-CaMP fluorescence intensity in AVA in an animal expressing *sraIs49 [nmr-1p::G-CaMP; unc-119(+)]*. The amplitude of G-CaMP fluorescence in AVA during reversals is $73 \pm 21\%$ (mean \pm SEM, 9 reversals), which is similar to that in AVA due to ASH activation in wild type ($P = 0.6$), *lite-1* ($P = 0.4$) and *osm-3* ($P = 0.3$) genetic backgrounds and due to RIM activation in wild type ($P = 0.3$) and *lite-1* ($P = 0.4$) genetic backgrounds (**Supplementary Fig. 5, 15**, Welch's t-test).

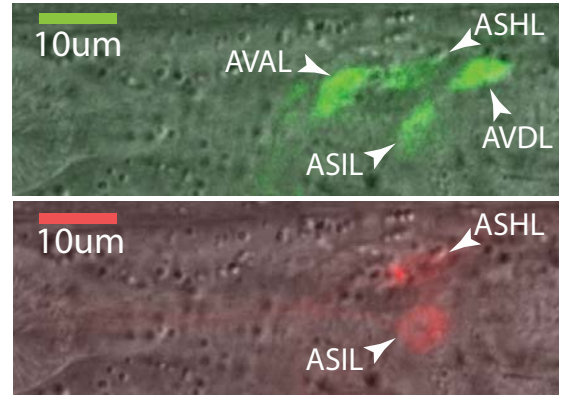
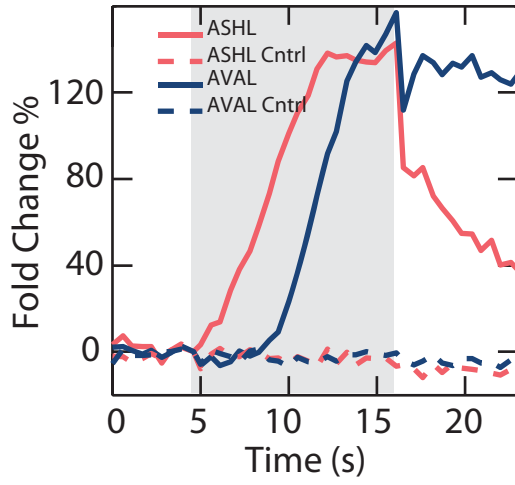
Supplementary Figure 2



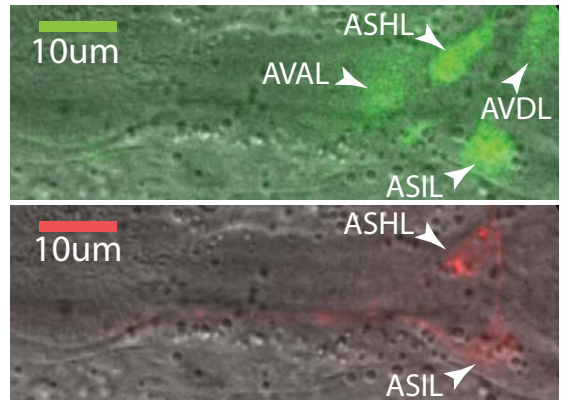
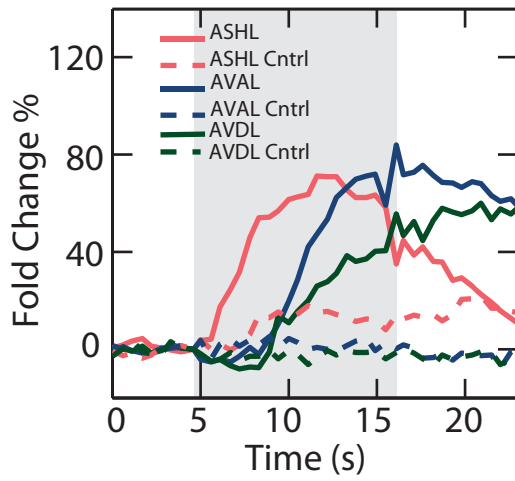
Supplementary Figure 3 | Low laser intensity, $0.01\text{mw}/\text{mm}^2$, can monitor G-CaMP fluorescence in AVA and AVD upon ASH activation. (a-d) The percentage change of G-CaMP fluorescence intensity as a function of time is plotted for ASH (pink solid line), AVA (dark blue solid line) and AVD (dark green solid line). For the control traces (dashed lines), stimulation light was not turned on. The grey region indicates the time period during which ASH was stimulated with the excitation light. The green and red channel images superposed on DIC (exactly as in **Fig. 4**) are shown in each sub-figure, for the animals from which the traces were recorded. Data from four different animals were shown. The low laser intensity used here can still monitor G-CaMP fluorescence of ASH with the signal above the noise background.

Supplementary Figure 3

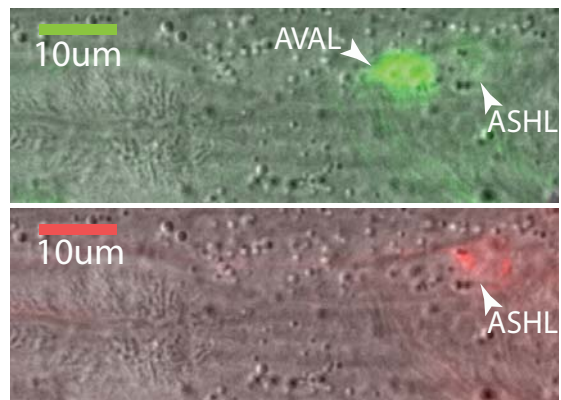
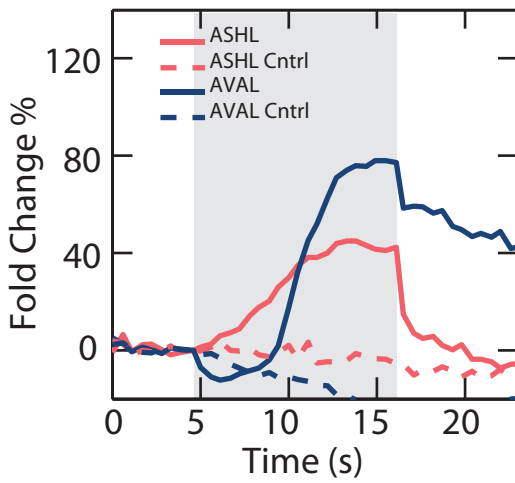
a



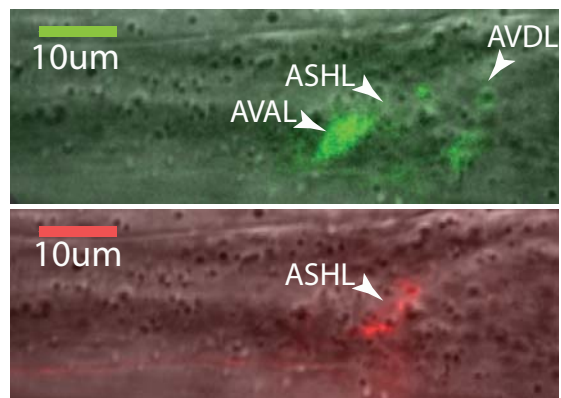
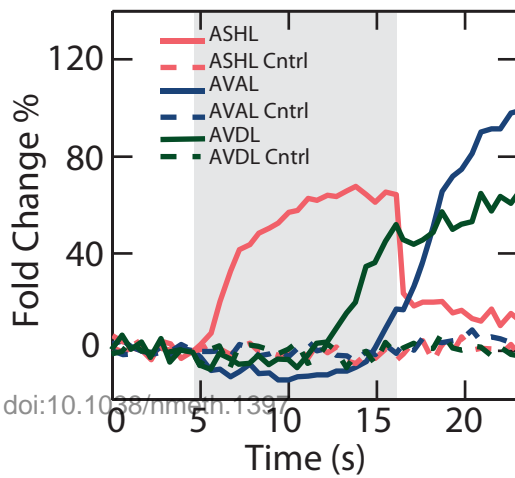
b



c



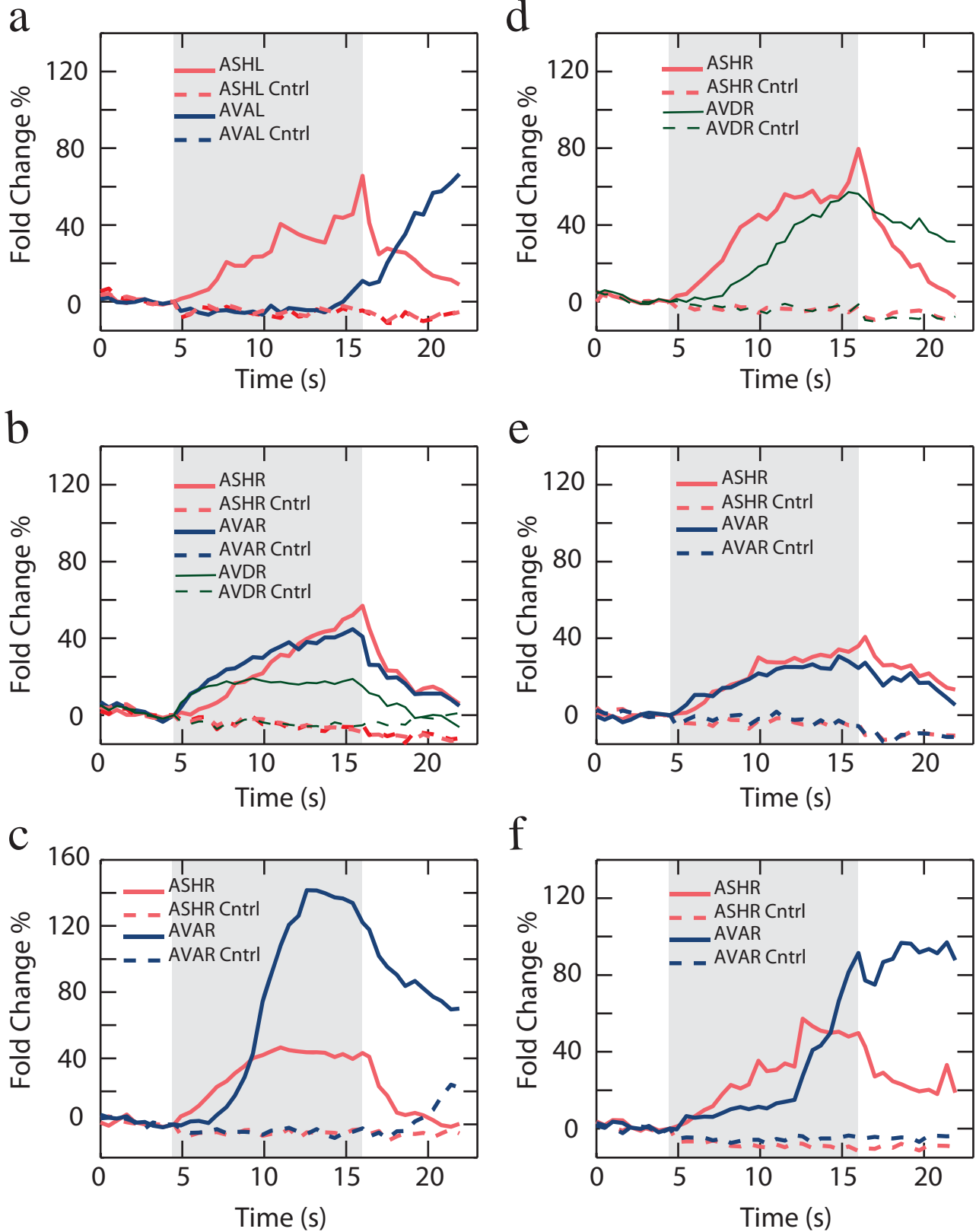
d



Supplementary Figure 4 | Specific stimulation of ASH activates AVA and AVD in *lite-1(ce314)* animals. The percentage change of G-CaMP fluorescence intensity as a function of time is plotted for ASH (pink solid line), AVA (dark blue solid line) and AVD (dark green solid line). The grey region indicates the time period during which ASH was stimulated with the excitation light. Data from six different animals were shown. 9 of the 10 animals examined showed AVA and/or AVD activity upon ASH stimulation.

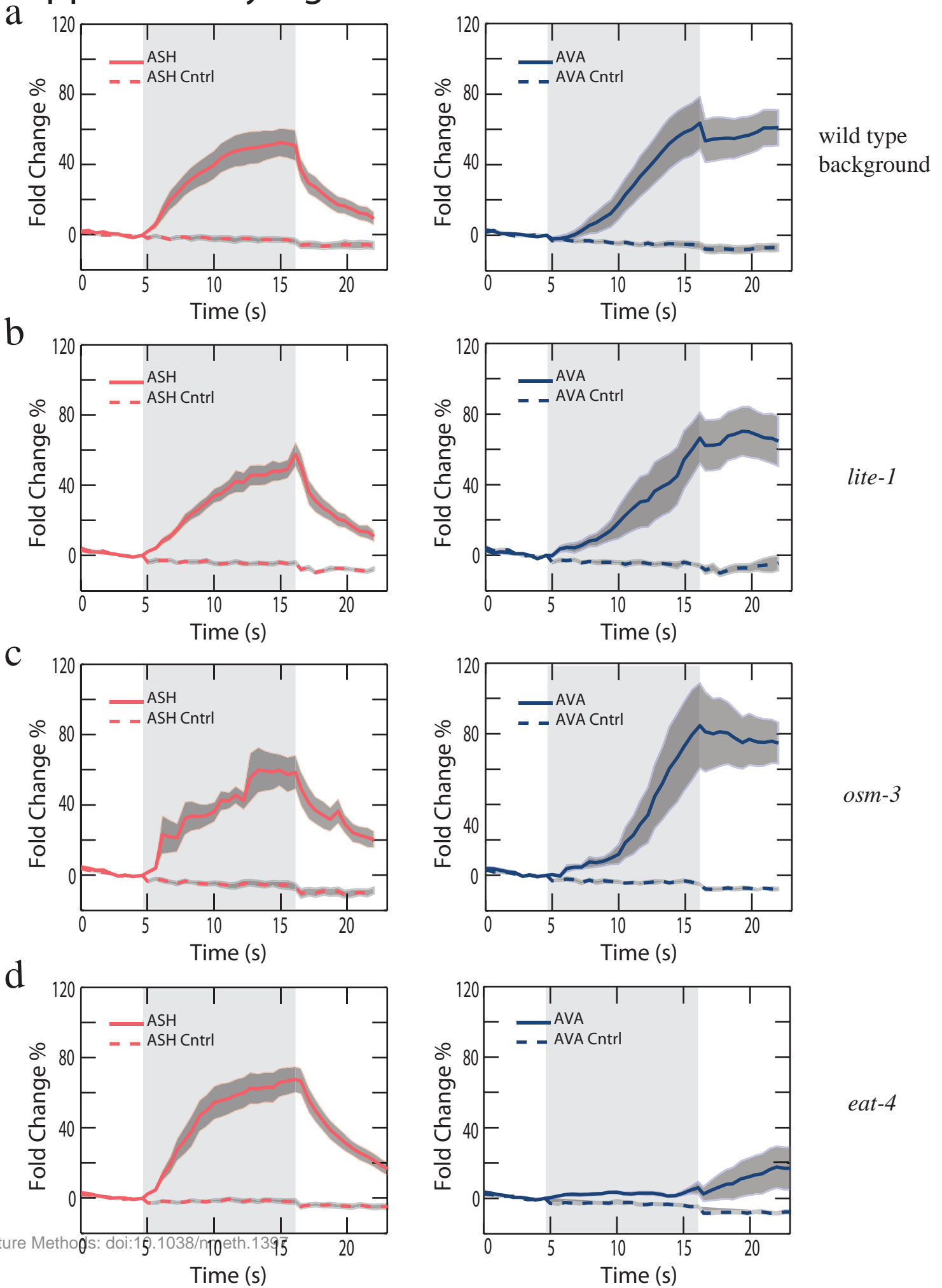
Supplementary Figure 4

lite-1



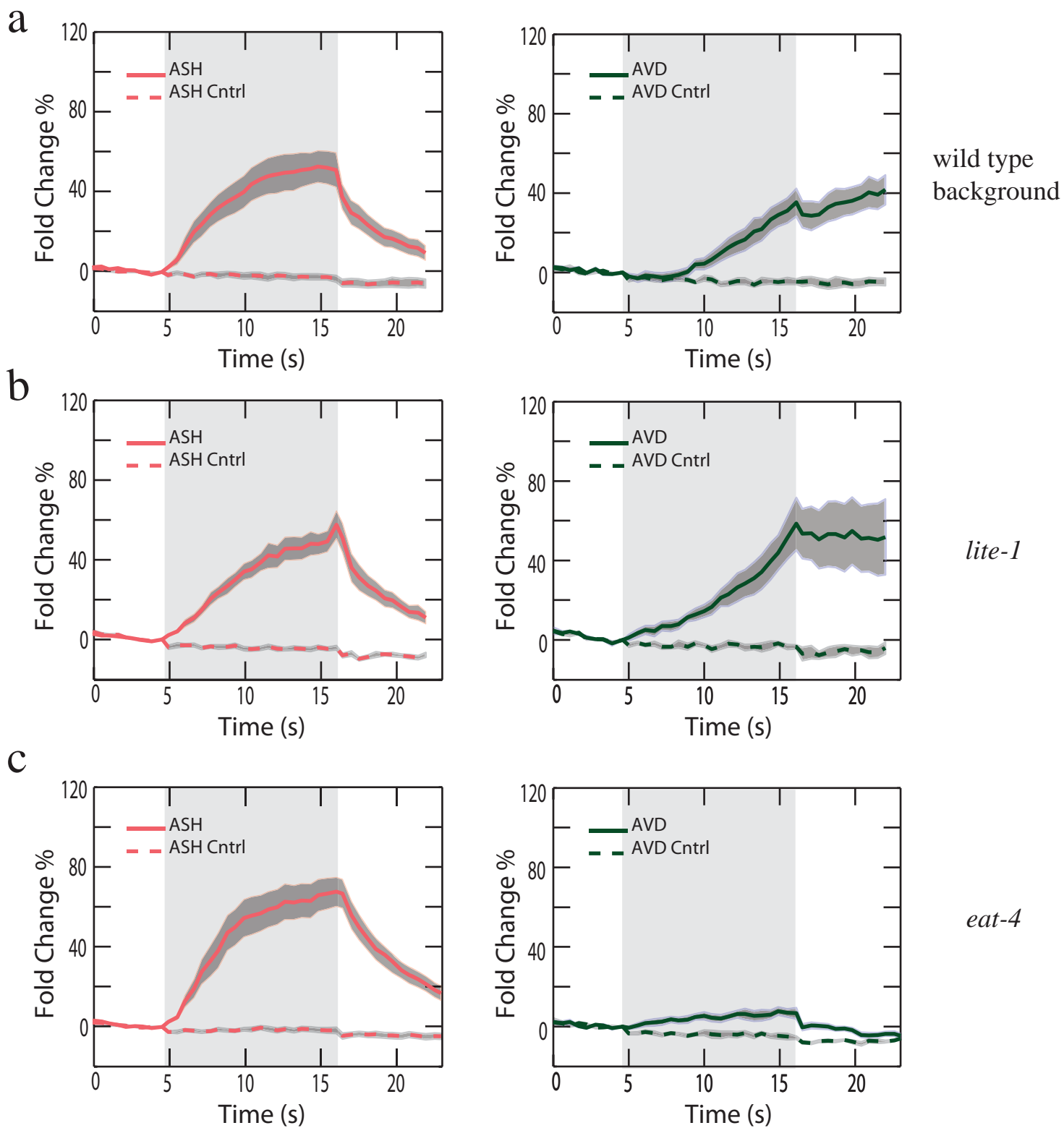
Supplementary Figure 5 | Averaged G-CaMP traces in ASH and AVA upon ASH stimulation in *lite-1*, the wild type, *osm-3* and *eat-4* genetic background. Traces represent averaged G-CaMP fluorescence in ASH and AVA. The grey region around each curve represents the standard error of the mean. The rectangular grey region indicates the time period during which ASH was stimulated. The amplitude of G-CaMP fluorescence in ASH due to ASH stimulation in *lite-1*, wild type, *osm-3* and *eat-4* genetic background is 59 ± 21 % ($n = 9$), 59 ± 32 % ($n = 14$), 74 ± 24 % ($n = 6$), and 74 ± 33 % ($n = 16$), respectively. The amplitude of G-CaMP fluorescence in AVA due to ASH stimulation in *lite-1*, wild type, *osm-3* and *eat-4* genetic background is 86 ± 38 % ($n = 8$), 81 ± 49 % ($n = 14$), 100 ± 50 % ($n = 6$) and 27 ± 45 % ($n = 16$). The amplitude of G-CaMP fluorescence in AVA due to ASH stimulation in *eat-4* genetic background is significantly different from that in *lite-1* ($P = 0.004$), wild type ($P = 0.004$) and *osm-3* ($P = 0.01$) genetic backgrounds (Welch's t-test). (a) Data from **Fig. 5a** and **Supplementary Fig. 4** and two additional animals that was not shown. (b) Data from **Fig. 5b**, **Supplementary Fig. 3, 8, 9a** and two additional animals that were not shown. (c) Data from **Supplementary Fig. 10**. (d) Data from **Fig. 5d, Supplementary Fig. 11** and seven additional animals that were not shown.

Supplementary Figure 5



Supplementary Figure 6 | Averaged G-CaMP traces in ASH and AVD upon ASH stimulation in the wild type, *lite-1* and *eat-4* genetic background. Traces represent averaged G-CaMP fluorescence in ASH and AVD. The grey region around each curve represents the standard error of the mean. The rectangular grey region indicates the time period during which ASH was stimulated. Averaged traces in ASH were shown in **Supplementary Fig. 5**. The amplitude of G-CaMP fluorescence in AVD due to ASH stimulation in wild type and *lite-1* and *eat-4* genetic background is $47 \pm 16\%$ ($n=7$), $69 \pm 34\%$ ($n = 5$) and $9 \pm 5\%$ ($n = 6$). The activation of AVD due to ASH stimulation in *eat-4* worms is significantly different from that in wild type ($P = 0.0006$) and *lite-1* ($P = 0.017$) worms (Welch's t-test). **(a)** Data from **Fig. 5b** and **Supplementary Fig. 3, 8** and one additional animal that was not shown. **(b)** Data from **Fig. 5a**, **Supplementary Fig. 4** and two additional animals that was not shown. **(c)** Data from **Fig 5d**, **Supplementary Fig. 11** and three additional animals that were not shown.

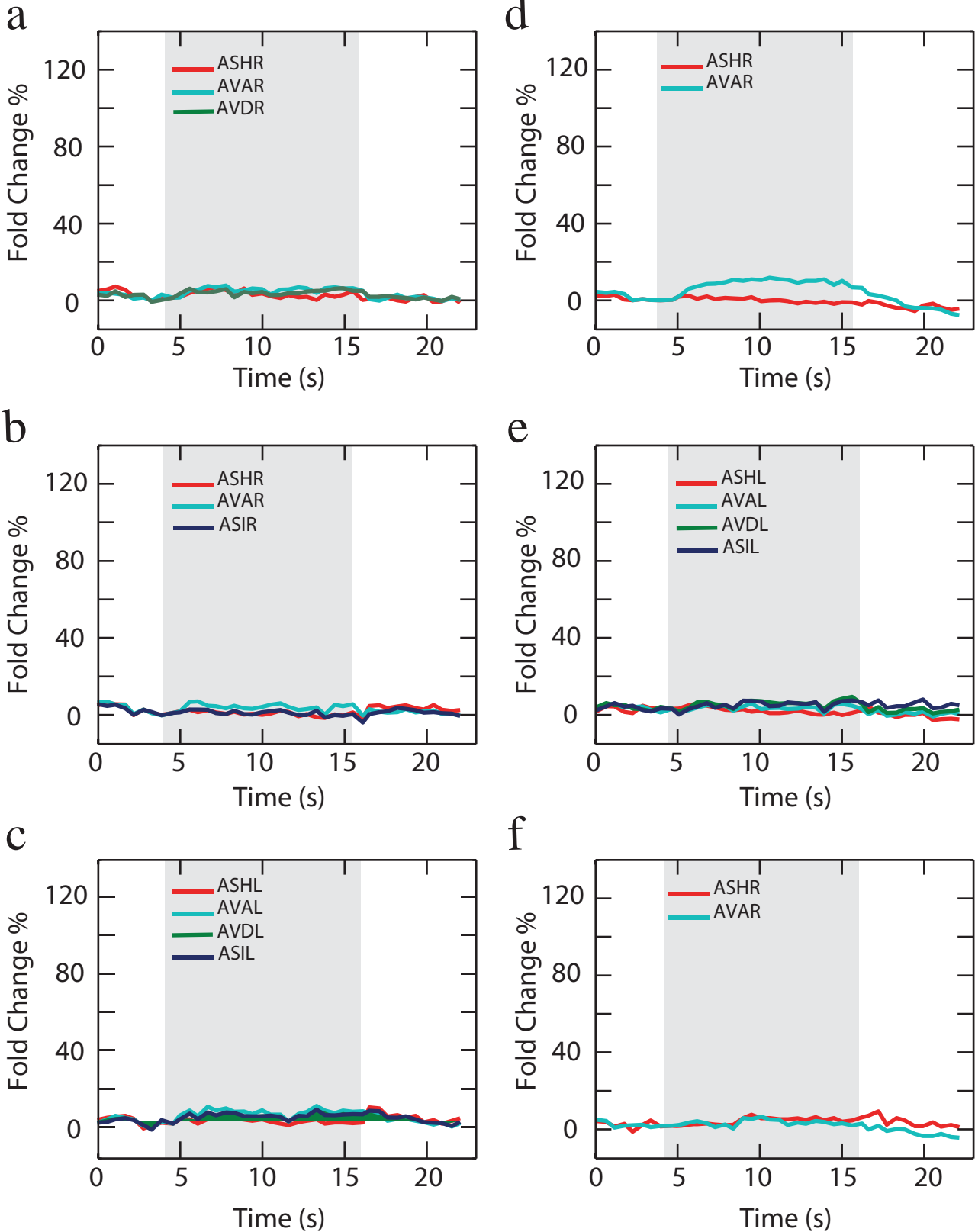
Supplementary Figure 6



Supplementary Figure 7 | Specific stimulation of ASH in *lite-1(ce314)* animals cultivated without retinal resulted no activation in both ASH and AVA. The percentage change of G-CaMP fluorescence intensity as a function of time is plotted for ASH (dark magenta solid line), AVA (light blue solid line), AVD (dark green solid line), and ASI (dark blue solid line). The grey region indicates the time period during which ASH was stimulated with the excitation light. Data from six different animals were shown. None of the 6 animals examined showed AVA and/or AVD activity upon ASH stimulation. Animals cultivated without retinal in *osm-3* mutant animals (n=6) were also examined and none of them showed AVA and/or AVD activity upon ASH stimulation.

Supplementary Figure 7

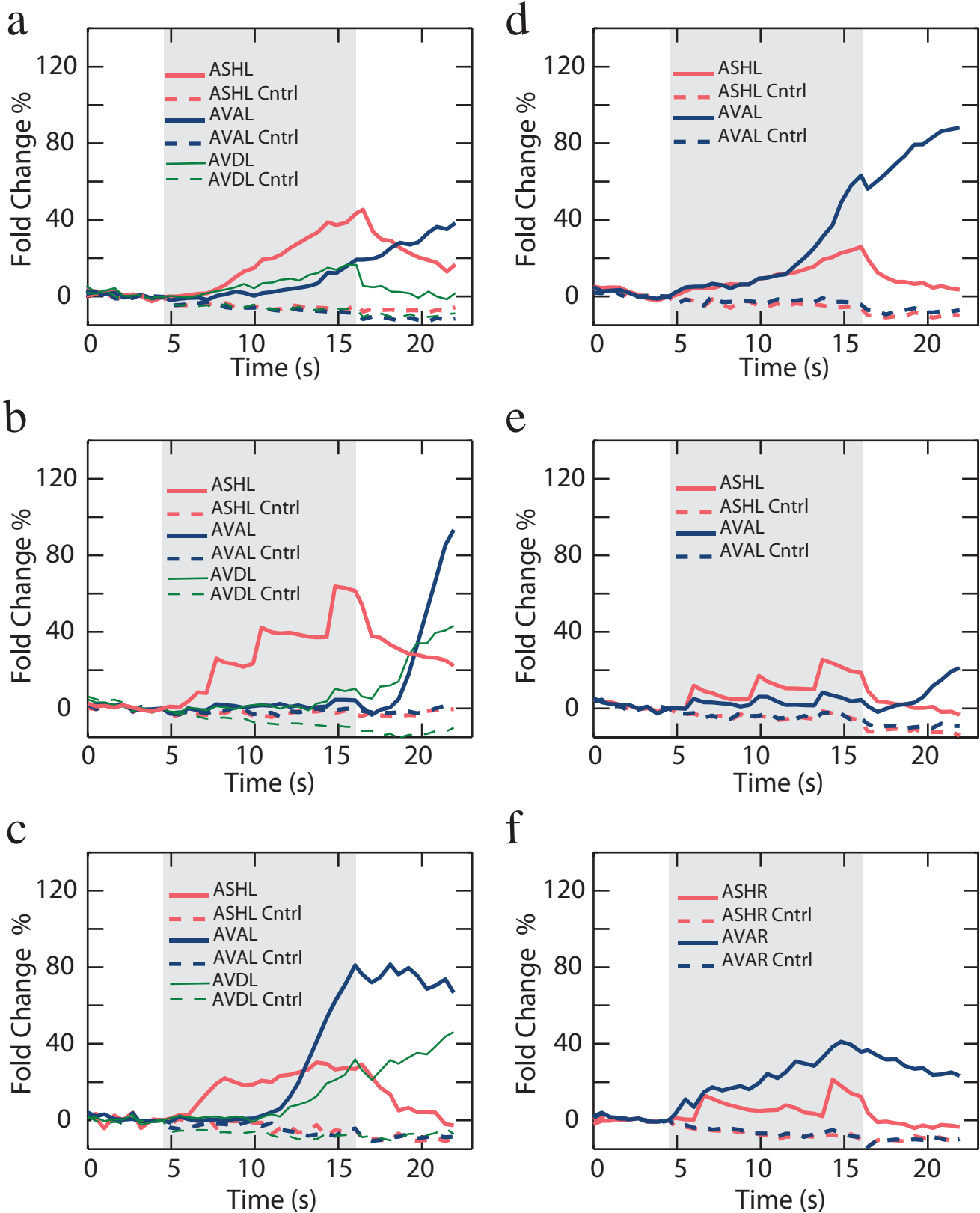
lite-1, no Retinal



Supplementary Figure 8 | Specific stimulation of ASH activates AVA and AVD in the wild type background. The percentage change of G-CaMP fluorescence intensity as a function of time is plotted for ASH (pink solid line), AVA (dark blue solid line) and AVD (dark green solid line). The grey region indicates the time period during which ASH was stimulated with the excitation light. Data from six different animals were shown. 8 of the 10 animals examined showed AVA and/or AVD activity upon ASH stimulation.

Supplementary Figure 8

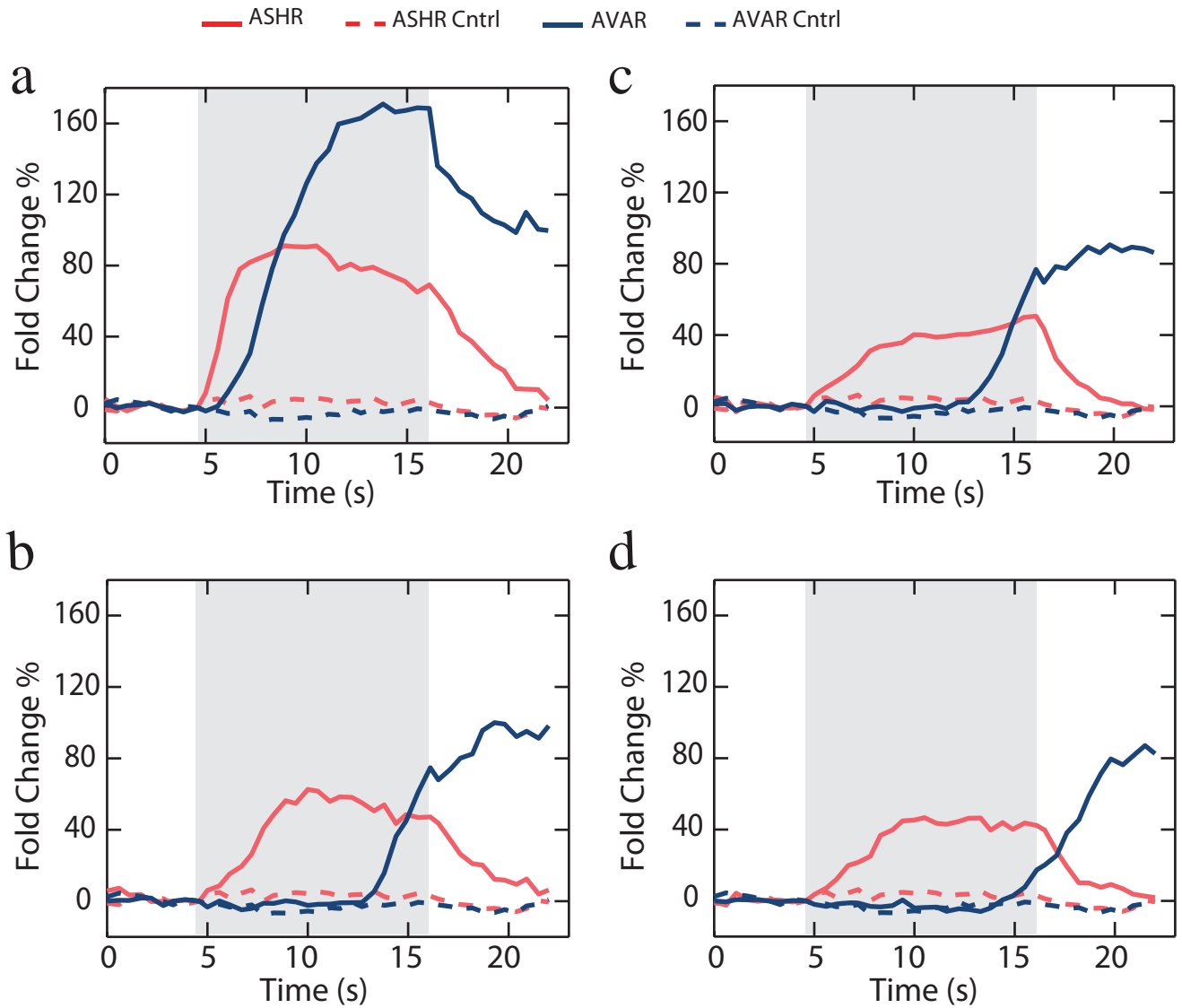
WT background



Supplementary Figure 9 | Stimulation of ASH can repeatedly activate AVA in the wild type background. The percentage change of G-CaMP fluorescence intensity as a function of time is plotted for ASH (pink solid line) and AVA (dark blue solid line). The grey region indicates the time period during which ASH was stimulated with the excitation light. The first (**a**), second (**b**), third (**c**) and fourth (**d**) stimulation results show robust responses in AVA upon ASH stimulation. The intensity of the 488nm laser used to monitor G-CaMP fluorescence was about 0.01mW/mm².

Supplementary Figure 9

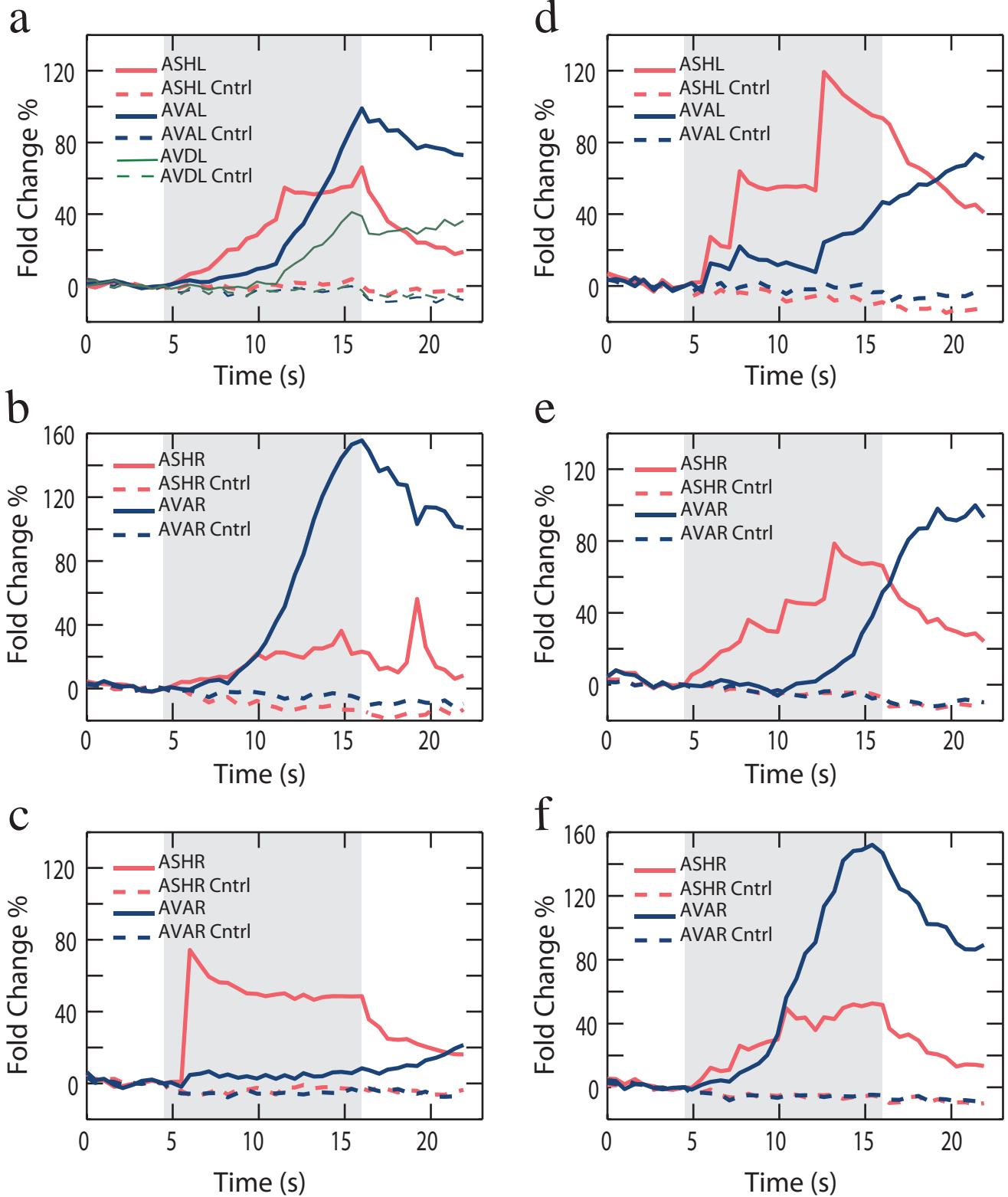
WT background



Supplementary Figure 10 | Specific stimulation of ASH activates AVA and AVD in the *osm-3(p802)* background. The percentage change of G-CaMP fluorescence intensity as a function of time is plotted for ASH (pink solid line), AVA (dark blue solid line) and AVD (dark green solid line). The grey region indicates the time period during which ASH was stimulated with the excitation light. Data from six different animals were shown. All of the 8 animals examined showed AVA and/or AVD activity upon ASH stimulation. The traces in (a) was from **Fig. 5c**.

Supplementary Figure 10

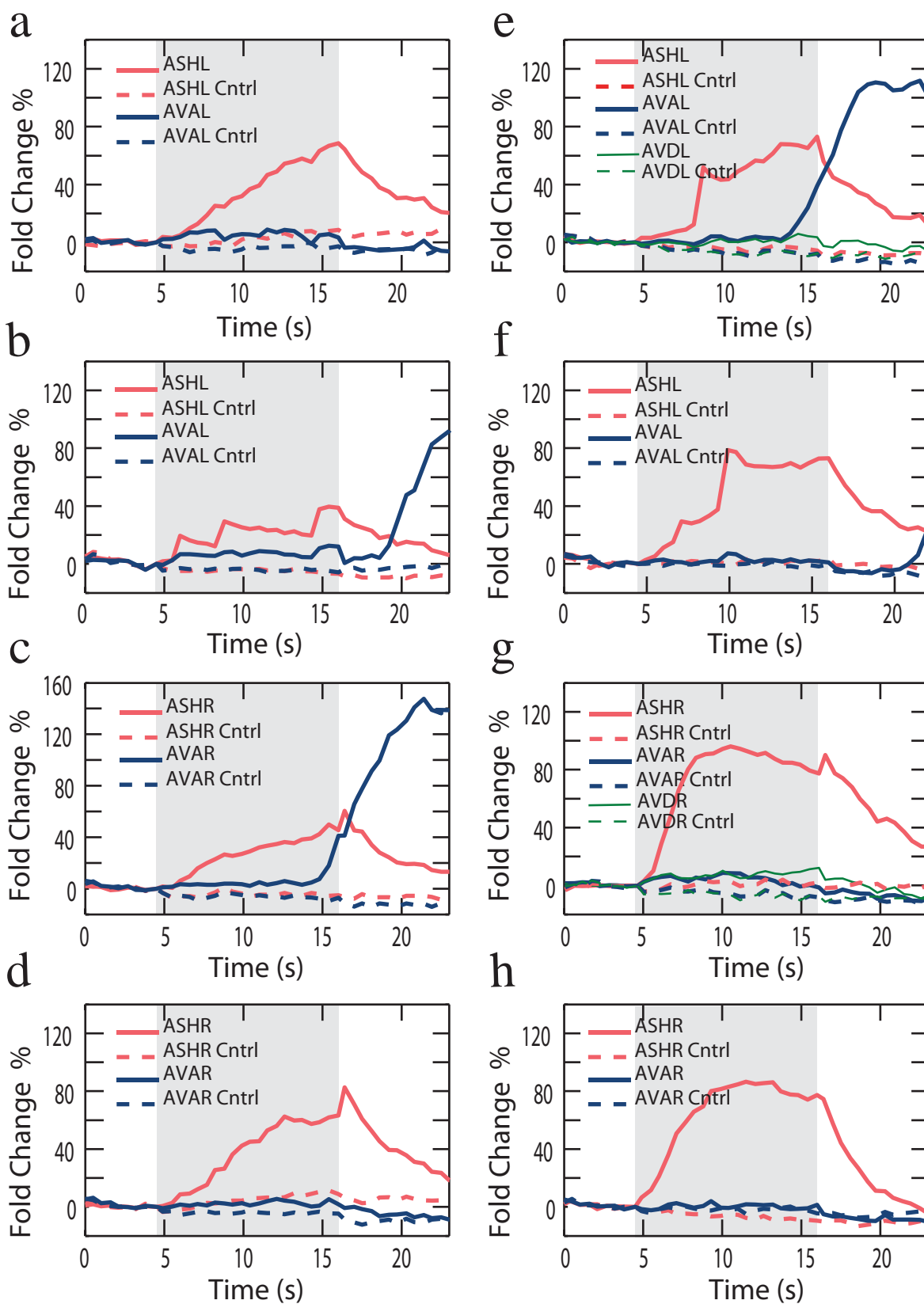
osm-3



Supplementary Figure 11 | Specific stimulation of ASH typically can not activate AVA and AVD in the *eat-4(ky5)* background. The percentage change of G-CaMP fluorescence intensity as a function of time is plotted for ASH (pink solid), AVA (dark blue solid line) and AVD (dark green solid line). The grey region indicates the time period during which ASH was stimulated with the excitation light. Data from eight different animals were shown. 5 of the 16 animals examined showed AVA and/or AVD activity upon ASH stimulation.

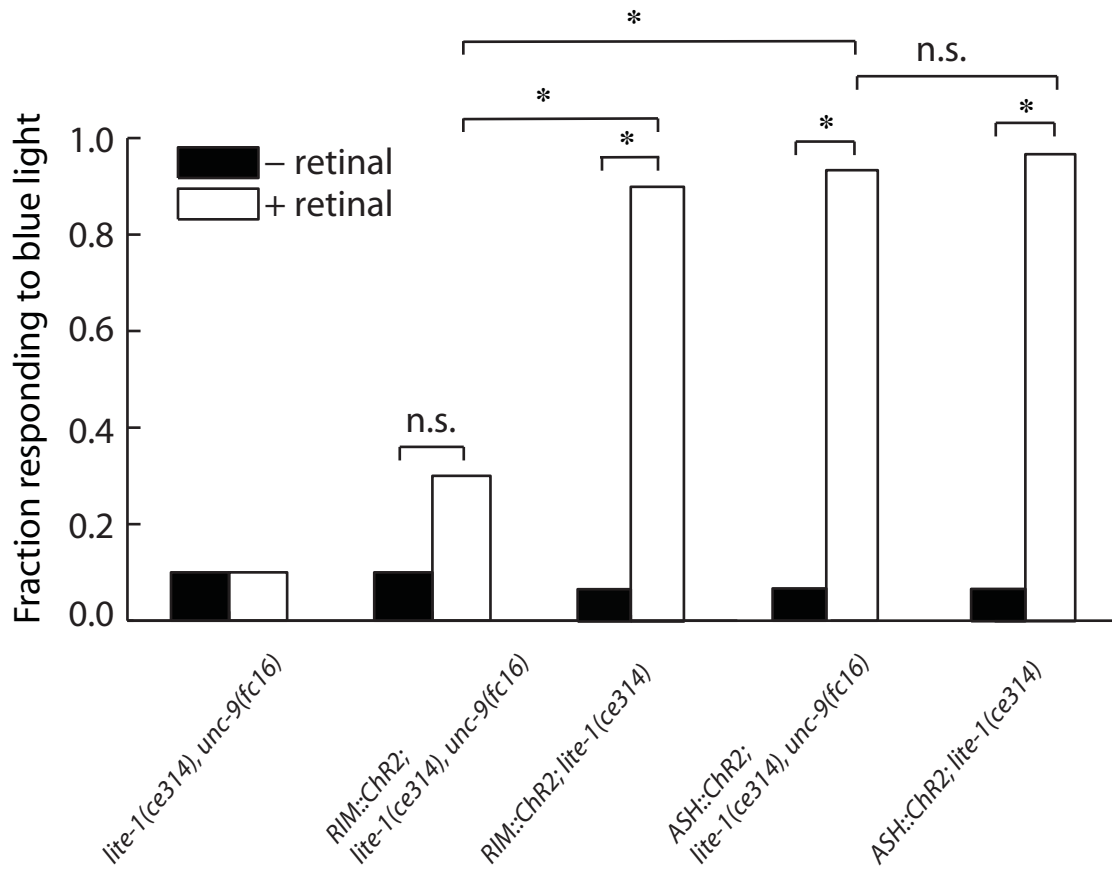
Supplementary Figure 11

eat-4



Supplementary Figure 12 | Behavior analysis of ChR2 activation in RIM/ASH in *lite-1(ce314), unc-9(fc16)* genetic background. In *unc-9(fc16)* genetic background, the avoidance response due to RIM activation was greatly reduced. However, in the same genetic background, the avoidance response due to ASH activation, liking the anterior touch response, was not greatly affected. The results indicate that RIM neurons predominately use gap junctions to activate AVA. Thirty animals were tested for each genetic background in the presence or absence of retinal. The standard chi-square test was used to determine the significance of the data. *RIM::ChR2* represents *tdc-1p::ChR2* and *ASH::ChR2* represents *sra-6p::ChR2*. * $p < 0.001$.

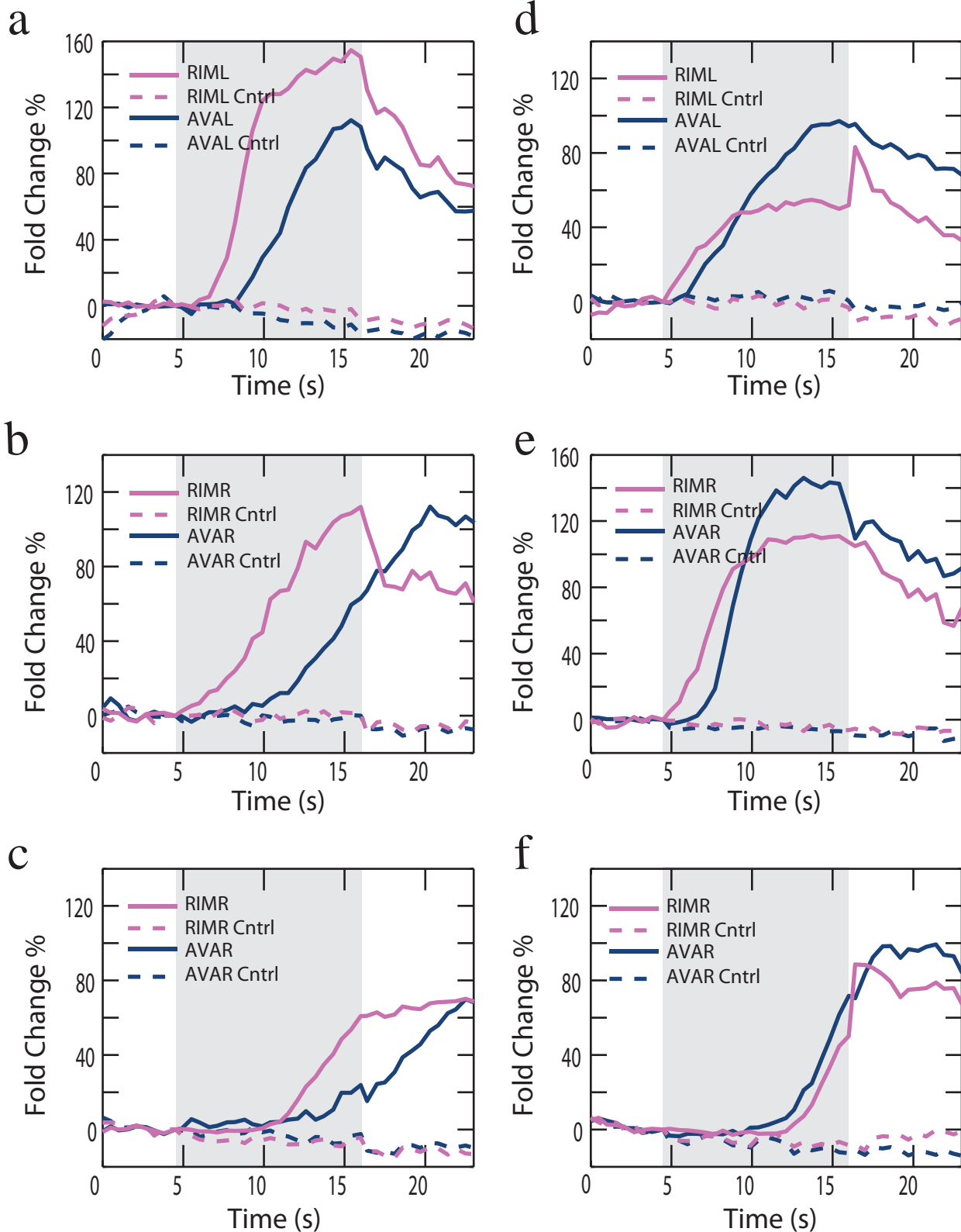
Supplementary Figure 12



Supplementary Figure 13 | Specific stimulation of RIM activates AVA in the wild type background. The percentage change of G-CaMP fluorescence intensity as a function of time is plotted for RIM (light magenta solid line) and AVA (dark blue solid line). The grey region indicates the time period during which RIM was stimulated with the excitation light. Data from six different animals were shown. All 8 animals that showed RIM activation also showed AVA activity.

Supplementary Figure 13

WT background

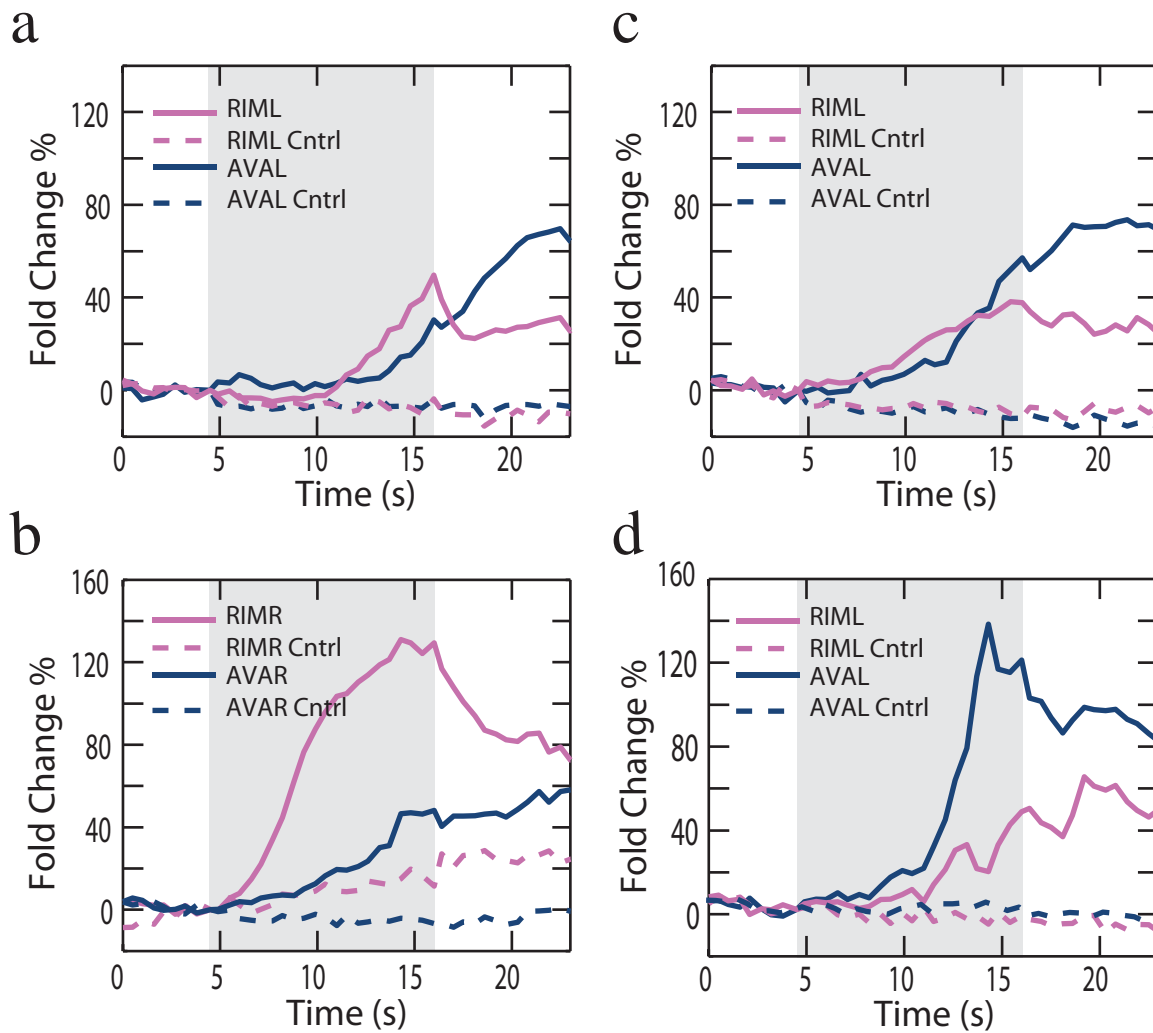


Supplementary Figure 14 | Specific stimulation of RIM activates AVA in the *lite-1(ce314)*

background. The percentage change of G-CaMP fluorescence intensity as a function of time is plotted for RIM (light magenta solid line) and AVA (dark blue solid line). The grey region indicates the time period during which RIM was stimulated with the excitation light. Data from six different animals were shown. All 5 animals that showed RIM activation also showed AVA activity.

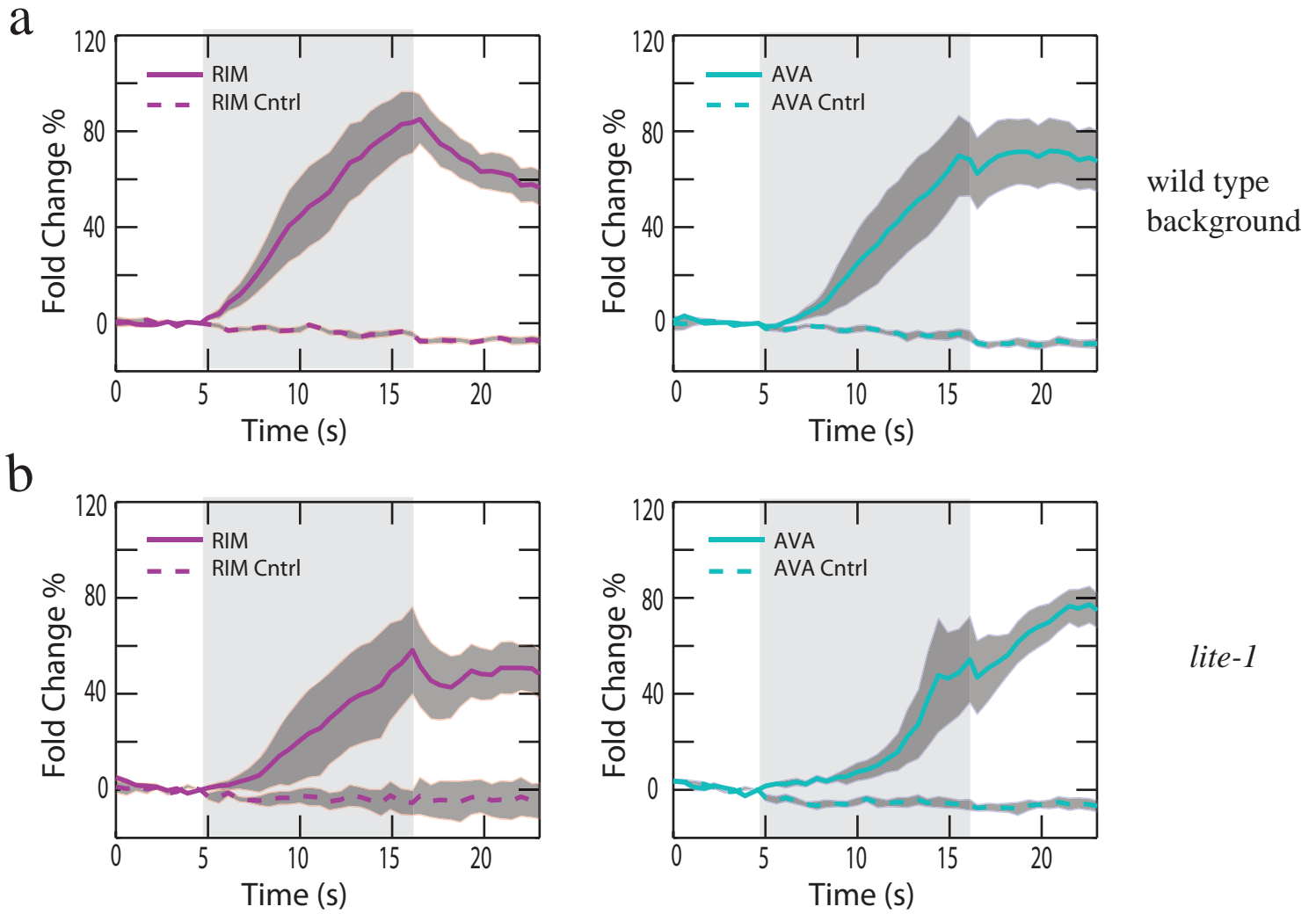
Supplementary Figure 14

lite-1



Supplementary Figure 15 | Averaged G-CaMP traces in RIM and AVA upon RIM stimulation in wild type and *lite-1(ce314)* genetic background. Traces represent averaged G-CaMP fluorescence in RIM and AVA. The grey region around each curve represents the standard error of the mean. The rectangular grey region indicates the time period during which ASH was stimulated. The amplitude of G-CaMP fluorescence in RIM due to RIM stimulation in wild type and *lite-1* genetic background is 95 ± 31 % ($n = 8$), 70 ± 36 % ($n = 5$) respectively. The amplitude of G-CaMP fluorescence in AVA due to RIM stimulation in wild type and *lite-1* genetic background is 90 ± 43 % ($n = 8$), 87 ± 32 % ($n = 5$) respectively. **(a)** Data from **Fig. 6b** and **Supplementary Fig. 13** and one additional animal that was not shown. **(b)** Data from **Fig. 6c** and **Supplementary Fig. 14**.

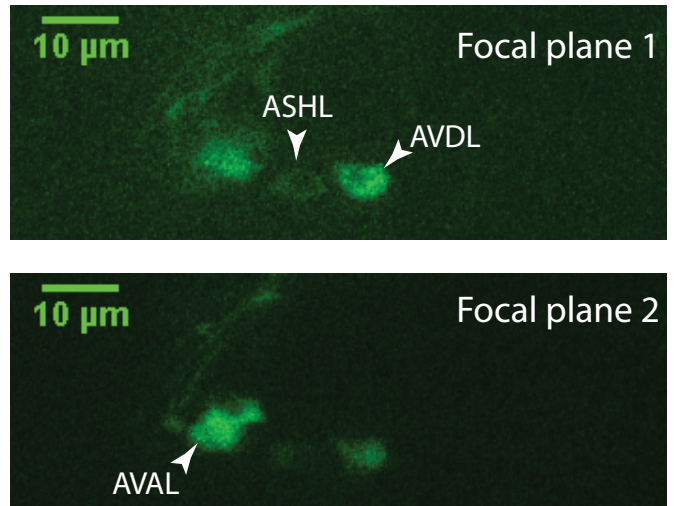
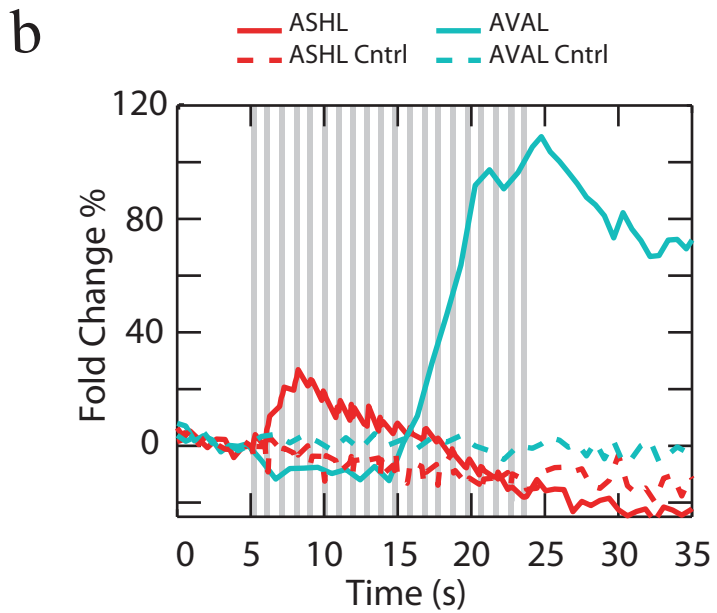
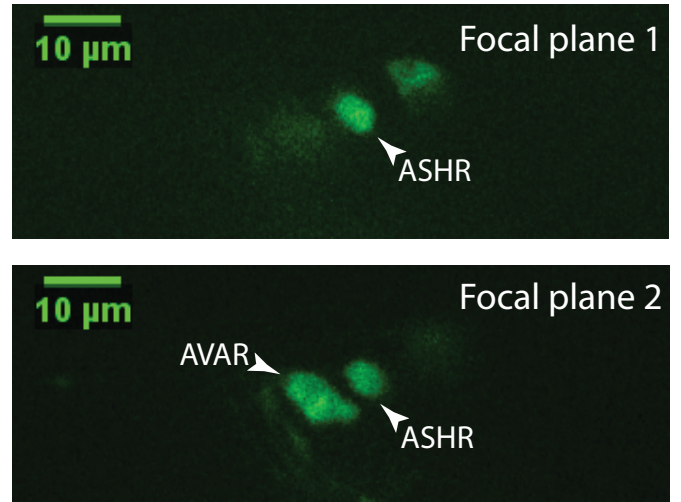
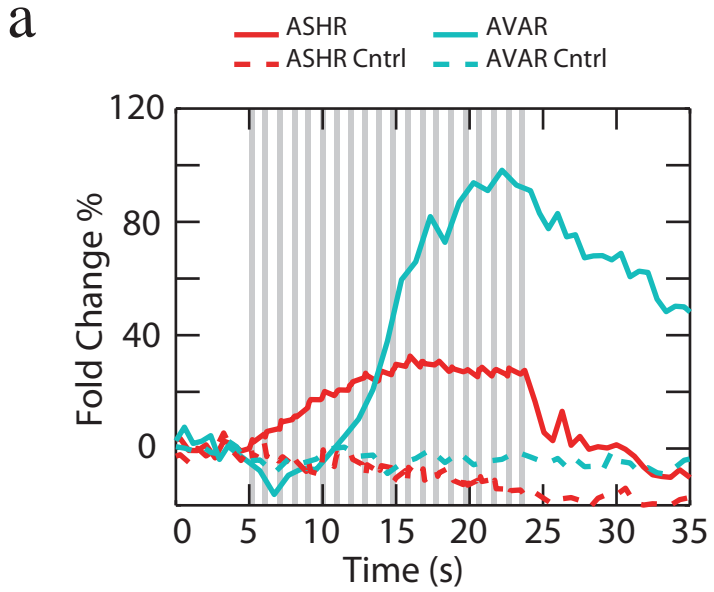
Supplementary Figure 15



Supplementary Figure 16 | Stimulating and monitoring neurons on different focal planes.

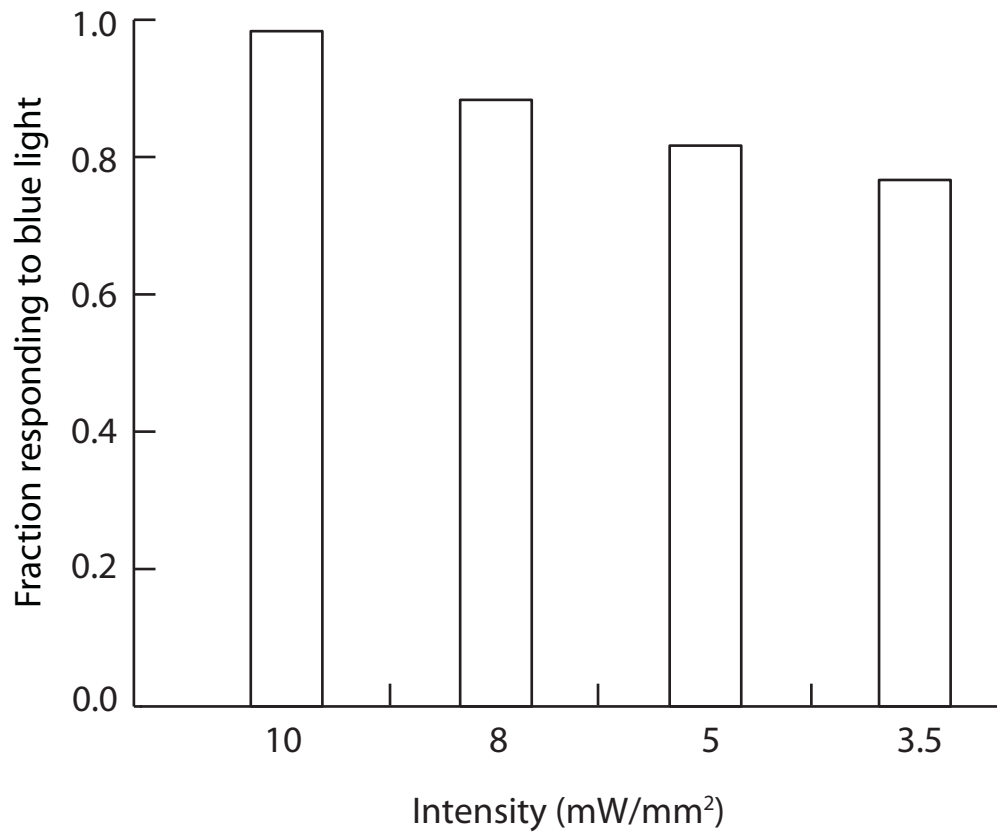
The percentage change of G-CaMP fluorescence intensity as a function of time is plotted for ASH (red) and AVA (light blue) in two different animals. The grey region indicates the time period during which ASH was stimulated with the excitation light. The total stimulation time is about 8 seconds. A piezo drive was used to switch focal planes in 10msec. Stimulating ChR2 in ASH was in focal plane 1; monitoring G-CaMP fluorescence in AVA was in focal plane 2. The two focal planes were about 10 μ m apart. The intensity of the 488nm laser used to monitor G-CaMP fluorescence was about 0.01mW/mm².

Supplementary Figure 16



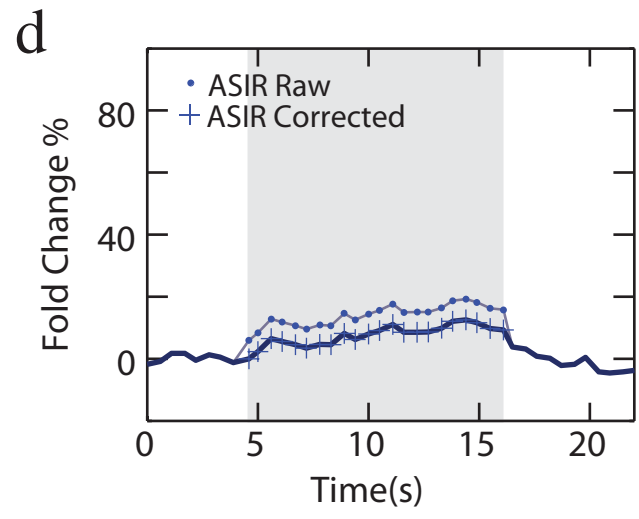
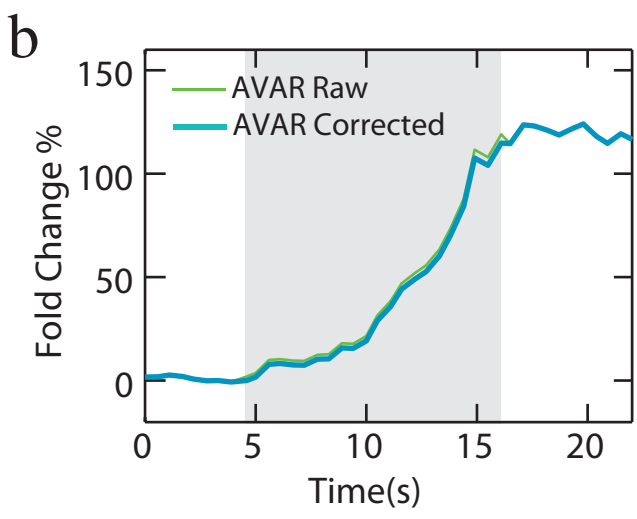
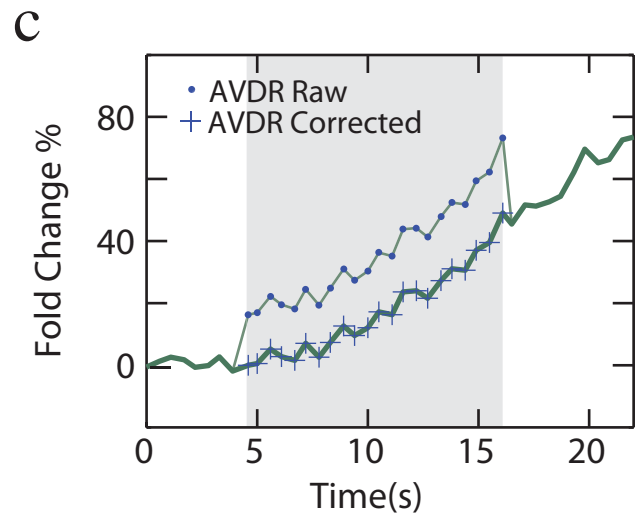
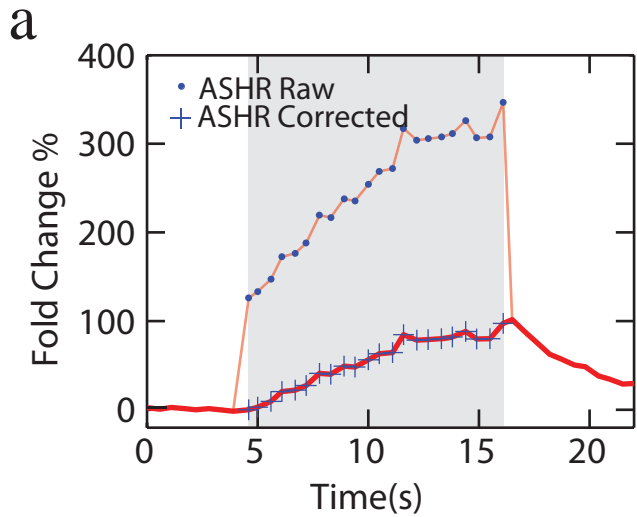
Supplementary Figure 17 | The avoidance response generated by ChR2 activation in ASH in *lite-1(ce314)* background is blue light intensity dependent. Fraction of animals that withdraw in response to blue light illumination is shown for different intensities. This fraction reaches 90% at around 8mW/mm².

Supplementary Figure 17



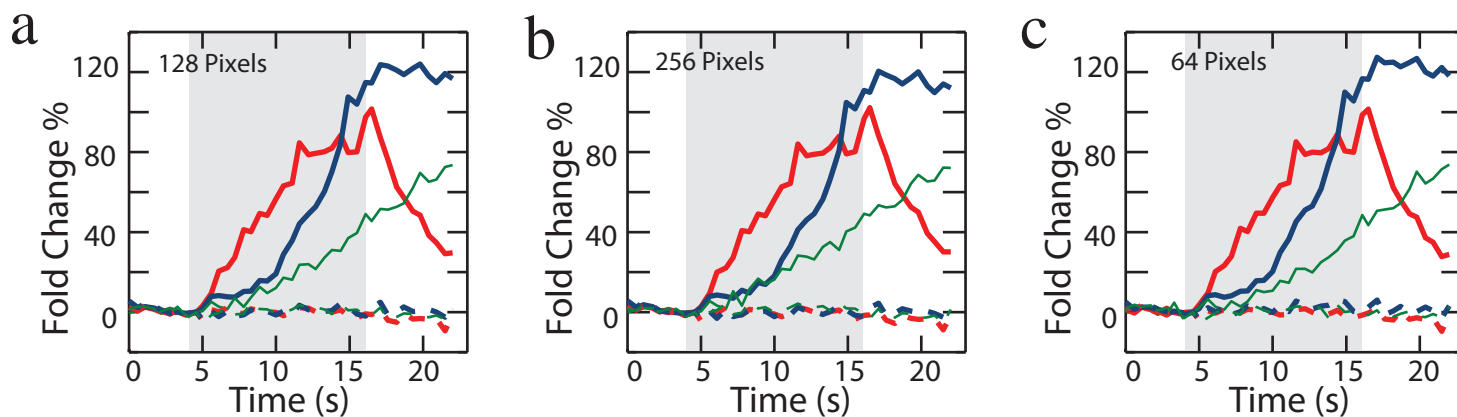
Supplementary Figure 18 | The G-CaMP fluorescence intensity jump in neurons stimulated using blue light. When a neuron expressing ChR2 was stimulated using blue light from the stimulation light path, there was a fluorescence intensity jump as the blue light used for stimulation also excites G-CaMP (**Fig. 4b, Supplementary Movies 3,4,6**). To correct this, the percentage change in fluorescence intensity during the stimulation period was scaled by a constant. The constant was determined by taking the instantaneous fold change in the fluorescence intensity upon stimulation (**Supplementary Methods**). In this way, the artificial jump was removed. The traces of ASHR, AVAR, AVDR and ASIR shown here are from **Fig.5a**.

Supplementary Figure 18



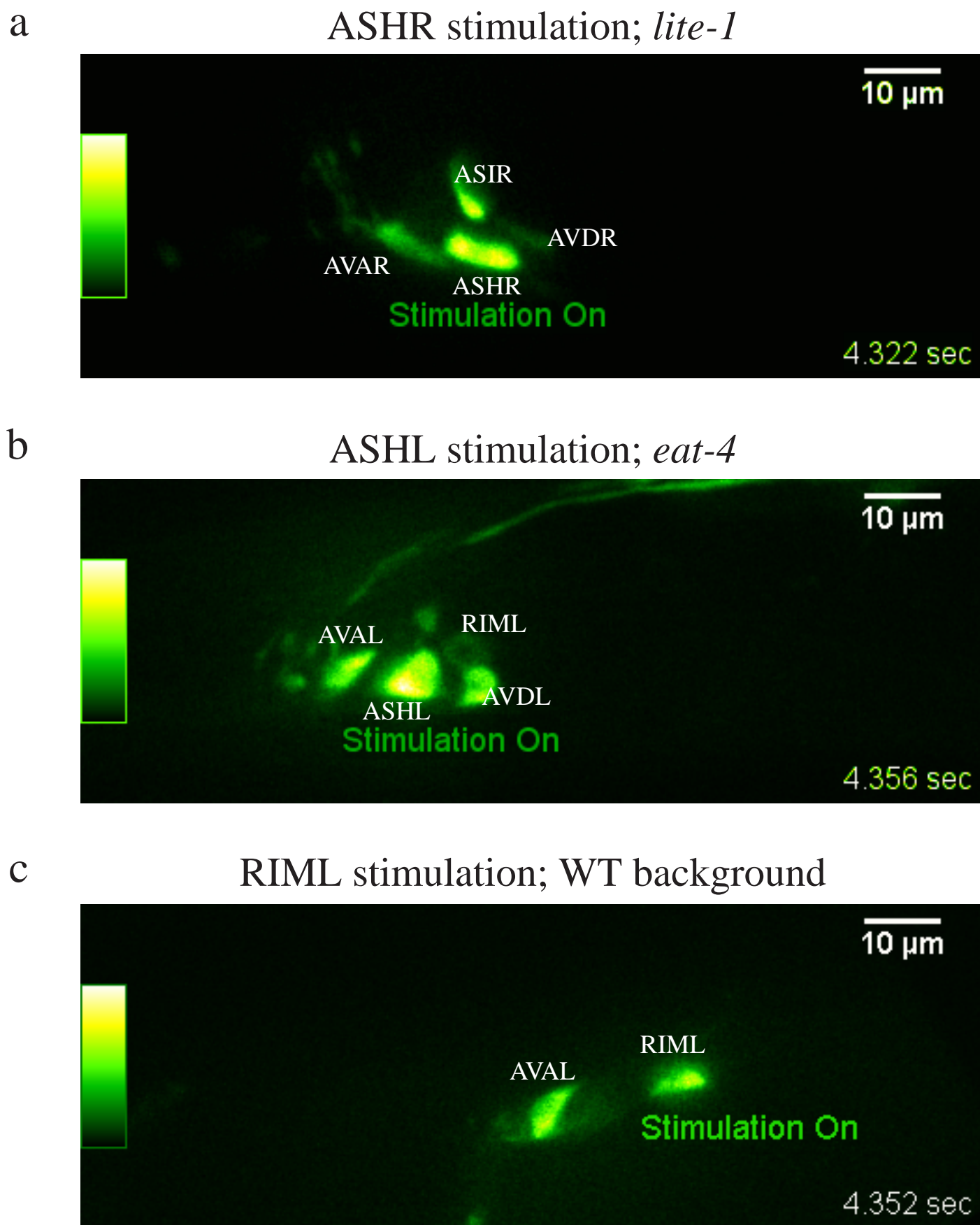
Supplementary Figure 19 | Effects of choosing different number of pixels on the G-CaMP fluorescence trace. When different number of pixels is chosen to calculate the percentage of fluorescence change, the results are almost the same. We used 128 pixels for all the fluorescence traces if not indicated. The traces of ASHR, AVAR and AVDR, shown here are from **Fig. 5a**.

Supplementary Figure 19



Supplementary Figure 20 | Illustration of movies. Single frames from **Supplementary Movies 3, 4 and 6** are shown. The stimulation light was just turned on in each frame as indicated by ‘stimulation on’. In each frame, anterior is at left and posterior at right.

Supplementary Figure 20



Supplementary Table 1 | Transgenic strains and their genotypes.

Name	Genotype
SRS47	<i>sraEx47 [nmr-1p::G-CaMP; unc-119(+)]; unc-119 (ed3)</i> III
SRS49	<i>sraIs49 [nmr-1p::G-CaMP; unc-119(+)]</i> V
SRS80	<i>sraIs49; sraEx80 [sra-6p::chop-2(H134R)::mCherry; osm-10p::G-CaMP; unc-122p::mCherry]</i>
SRS83	<i>sraEx83 [tdc-1p::chop-2(H134R)::mCherry; F55B11.3p::mCherry]</i>
SRS85	<i>sraIs49; sraEx80; lite-1(ce314)</i> X
SRS86	<i>sraIs49; sraEx83; lite-1(ce314)</i> X
SRS91	<i>sraIs49; lite-1(ce314)</i> X
SRS92	<i>sraIs49; sraEx80; osm-3(p802)</i> IV
SRS93	<i>sraIs49; sraEx80; eat-4(ky5)</i> III
SRS95	<i>sraIs49; sraEx80; osm-9(ky10)</i> IV
SRS97	<i>lite-1(ce314) unc-9(fc16)</i> X
SRS100	<i>sraIs49; sraEx83; tdc-1(n3419)</i> II; <i>lite-1(ce314)</i> X
SRS118	<i>sraEx83; lite-1(ce314) unc-9(fc16)</i> X
SRS119	<i>sraEx80; lite-1(ce314) unc-9(fc16)</i> X

Supplementary Table 2 | Primers used for PCR.

Purpose	Primers
<i>sra-6p</i>	5'-ctgtcatggcagcatttgagaag-3' and 5'-ggcaaatctgaaataataatattaaattctgcg-3'
<i>unc-122p</i>	5'-cccgctgataaattgtacgttacatctc-3' and 5'-gattgtgagccaatgaagtaaaatttc-3'
<i>tdc-1p</i>	5'-aaggagagagcattgcagtggttg-3' and 5'-ttggcggctcctgaaaaatgcacc-3'
<i>F55B11.3p</i>	5'-cccagtggaatgctctgaaattaaca-3' and 5'-atattcagcattggatttggtgtgag-3'
<i>tdc-1</i> deletion	5'- gttgatgctgcctattccggttcg-3' and 5'- ctctctcctcagcgcacacgc-3'

Supplementary Note

AVA response in *eat-4* mutant animals upon ASH stimulation

In the presence of retinal, about 30% of the *eat-4* mutant animals showed AVA activation upon ASH stimulation (**Supplementary Fig 11**). This is consistent with our behavioral data, where in the presence of retinal a significant fraction of *eat-4* mutant animals showed an avoidance response upon ChR2 activation in ASH (**Fig. 2**, $p < 0.01$). This may be due to signaling by glutamate in an *eat-4* independent manner, use of other neuro-transmitters or an activation of AVA by ASH through intermediate neurons. To calculate the response latency in each neuron, the standard deviation of the control traces without blue light stimulation, σ_0 , was calculated and $3\sigma_0$ was used as the threshold to detect a significant fluorescence change above background. As it is shown in **Supplementary Fig. 5**, the response of G-CaMP intensity in ASH to ASH stimulation in *eat-4* genetic background is similar to that in wild type, *lite-1*, *osm-3* genetic background; G-CaMP intensity in ASH in *eat-4* mutants reached the threshold in 2.3 ± 1.5 s ($n=16$), as compared to 2.5 ± 1.5 s ($n=14$) in wild type, 2.1 ± 0.8 s ($n=6$) in *lite-1*, 2.3 ± 1.2 s ($n=6$) in *osm-3* background. However, the response in AVA typically happened later in *eat-4* mutants; G-CaMP intensity in AVA in *eat-4* mutants reached the threshold in 14.3 ± 5.5 s ($n=5$, only the traces where the threshold was reached were counted, the intensity in over 60% of the worms never reached this threshold), which is slower than that in wild type background (7.0 ± 4.4 s, $n=14$, p -value <0.05), in *lite-1* background (5.0 ± 4.1 s, $n=6$, p -value <0.05) and in *osm-3* background (5.8 ± 3.7 s, $n=6$, p -value <0.05).

Comparison between the behavior assay and specific stimulation

Typically, animals responded to whole body blue light illumination by initiating backward movement within one second in the behavior assay (data not shown). However, it took about two seconds to detect a significant fluorescence rise in ASH when ASH was specifically stimulated (**Fig. 4, Supplementary Fig. 5, Supplementary Note**). Besides the difference in states of awake and anesthetized animals, several additional reasons might explain this discrepancy. First, the activation region was different in the behavior assay and the specific stimulation using the optical setup. In the behavior assay, animals were broadly illuminated and thus both the ASH soma and process in both sides of the animal were stimulated. While during stimulation using the optical setup, only the ASH soma in one side of the animal was stimulated and as a result, the stimulation level might be significantly less than that in behavior assay.

Second, the genetically encoded calcium sensor G-CaMP has limited sensitivity and slow kinetics (see Discussion in main text) and thus might delay the time at which we detect a significant fluorescence rise. The association time constant for G-CaMP1 is Ca^{2+} concentration dependent; it decreases from 0.23s at $0.2\mu\text{M Ca}^{2+}$ to 2.5ms at $1\mu\text{M Ca}^{2+}$ ⁵. In neurons, the resting intracellular cytosolic free Ca^{2+} concentration is typically less than $0.1\mu\text{M}$. During stimulation, Ca^{2+} concentration starts to increase from its resting level. Thus the association time constant is likely to be on the order of 1 second. In vivo experiments done in *Drosophila* motoneurons support this hypothesis; the association time constant is 0.84s for GCaMP1.3, 0.56s for GCaMP1.6 when 40Hz voltage pulse stimulation was used⁶; the association time constant is 1.38s for GCaMP1.6, 0.63s for GCaMP2 when 40Hz voltage pulse stimulation was used⁷. In our experiments, G-CaMP fluorescence in ASH increased significantly over background noise in about 2 seconds after ASH stimulation.

Supplementary References

1. Chen, B.L., Hall, D.H. & Chklovskii, D.B. Wiring optimization can relate neuronal structure and function. *Proc Natl Acad Sci U S A* **103**, 4723-8 (2006).
2. White, J.G., Southgate, E., Thomson, J.N. & Brenner, S. The structure of the nervous system of the nematode *Caenorhabditis elegans*. *Philos Trans R Soc Lond B Biol Sci* **314**, 1-340 (1986).
3. Hulme, S.E., Shevkoplyas, S.S., Apfeld, J., Fontana, W. & Whitesides, G.M. A microfabricated array of clamps for immobilizing and imaging *C. elegans*. *Lab Chip* **7**, 1515-23 (2007).
4. Chronis, N., Zimmer, M. & Bargmann, C.I. Microfluidics for in vivo imaging of neuronal and behavioral activity in *Caenorhabditis elegans*. *Nat Methods* **4**, 727-31 (2007).
5. Nakai, J., Ohkura, M. & Imoto, K. A high signal-to-noise Ca(2+) probe composed of a single green fluorescent protein. *Nat Biotechnol* **19**, 137-41 (2001).
6. Reiff, D.F. et al. In vivo performance of genetically encoded indicators of neural activity in flies. *J Neurosci* **25**, 4766-78 (2005).
7. Hendel, T. et al. Fluorescence changes of genetic calcium indicators and OGB-1 correlated with neural activity and calcium in vivo and in vitro. *J Neurosci* **28**, 7399-411 (2008).